Templated Droplets and Ordered Arrays in Polymer-Dispersed Liquid-Crystal Films

Brenda J. Luther, Gerald H. Springer, and Daniel A. Higgins*

Department of Chemistry, Kansas State University, Manhattan, Kansas 66506-3701

Received February 28, 2001. Revised Manuscript Received May 2, 2001

Well-ordered two-dimensional hexagonal arrays of micrometer-sized nematic liquid-crystal droplets are prepared in polymer films. Droplets of uniform sizes and shapes are formed by "prefabricating" the voids in which the liquid crystal is to be entrapped. Void preparation involves deposition of polystyrene microspheres on a substrate to form a colloidal crystal array. The array is coated with water-soluble polymer and dried. The microspheres were then extracted with organic solvent. The voids are refilled with liquid crystal by capillary filling. The materials are characterized throughout this process by atomic force and multiphoton-excited fluorescence microscopies. Polarization-dependent fluorescence images show well-ordered nematic configurations within each droplet. Surprisingly, the nematic alignment in neighboring droplets is often found to be correlated over large domains spanning several droplets. The origins of these organizational correlations are explored.

I. Introduction

Polymer-dispersed liquid-crystal (PDLC) films[1] are of current technological and fundamental interest.[2] Usually comprised of micrometer-sized droplets of nematic liquid crystal dispersed in an optically transparent polymer matrix, they find applications as electrically switchable windows and light shutters. The birefringent liquid-crystal droplets form light-scattering centers. Their scattering properties can be switched on and off by applying an electric field across the film. The switchable light-scattering properties of PDLCs provide optical contrast in window applications, while light shutters are produced by doping the liquid crystal with strongly absorbing dichroic dyes.[3] New applications of PDLCs that use alternative optical contrast mechanisms continue to be developed. For example, electrically switchable diffractive optics[4] have recently been fabricated. Such systems have utilized transient gratings prepared in photorefractive PDLCs[5] and permanent electrically switchable gratings prepared holographically during device fabrication.[6] Related materials have also been reported.[7]

In the vast majority of PDLC devices, droplet size and shape play an important role in determining film optical and electro-optical properties. Film light-scattering efficiency and its angular dependence are controlled by liquid-crystal droplet size.[8] In addition, droplet size and shape attributes help determine both the electric field strength required to induce liquid-crystal reorientation and the rate at which such reorientation occurs.[9,10] However, PDLC films are most often prepared by emulsion or phase-separation procedures in which droplet morphology is strictly uncontrolled.[11] Films with broad droplet size distributions and variable droplet shapes are obtained, often resulting in suboptimal optical and electro-optical properties. A primary goal of the present work is the demonstration of effective procedures for preparing PDLC films incorporating droplets of well-controlled, highly regular sizes and shapes. An additional goal is the fabrication of well-ordered arrays of liquid-crystal droplets for possible applications in electrically switchable diffractive optics. These materials are characterized by atomic force microscopy (AFM) and multiphoton-excited (MPE) fluorescence microscopy.[12,13] The latter method allows for excitation and detection of native liquid-crystal fluorescence and provides high-resolution, polarization-dependent optical images for detailed characterization of liquid-crystalline order and organization.

* To whom correspondence should be addressed. E-mail: higgins@ksu.edu.

(1) (a) Doane, J. W.; Vaz, N. A.; Wu, B.-G.; Zumer, S. *Appl. Phys. Lett.* **1986**, *48*, 269. (b) Drzaic, P. S. *J. Appl. Phys.* **1986**, *60*, 2142.

(2) (a) Crawford, G. P.; Doane, J. W.; Zumer, S. in *Handbook of Liquid Crystal Research*; Collings, P. J., Patel, J. S., Eds. Oxford University Press: New York, 1997; pp 347−414. (b) Higgins, D. A. *Adv. Mater.* **2000**, *12*, 251.

(3) Drzaic, P. S. *Pure Appl. Chem.* **1996**, *68*, 1435.

(4) Park, S. H.; Xia, Y. *Langmuir* **1999**, *15*, 266.

(5) (a) Golemme, A.; Kippelen, B.; Peyghambarian, N. *Appl. Phys. Lett.* **1998**, *73*, 2408. (b) Wiederrecht, G. P.; Wasielewski, M. R. *J. Am. Chem. Soc.* **1998**, *120*, 3231. (c) Ono, H.; Kawatsuki, N. *Opt. Lett.* **1997**, *22*, 1144.

(6) Bunning, T. J.; Natarajan, L. V.; Tondiglia, V. P.; Sutherland, R. L. *Annu. Rev. Mater. Sci.* **2000**, *30*, 83.

(7) (a) Yoshino, K.; Shimoda, Y.; Kawagishi, Y.; Nakayama, K.; Ozaki, M. *Appl. Phys. Lett.* **1999**, *75*, 932. (b) Kim, M.-H.; Kang, W.-S.; Kim, J.-D. *Mol. Cryst. Liq. Cryst.* **2000**, *349*, 127.

(8) (a) Montgomery, G. P.; West, J. L.; Tamura-Lis, W. *J. Appl. Phys.* **1991**, *69*, 1605. (b) Van De Hulst, H. C. *Light Scattering by Small Particles*; John Wiley and Sons: New York, 1957. (c) Whitehead, J. B.; Zumer, S.; Doane, J. W. *J. Appl. Phys.* **1993**, *73*, 1057.

(9) Drzaic, P. S. *Liq. Cryst.* **1988**, *3*, 1543.

(10) Erdmann, J.; Doane, J. W.; Zumer, S.; Chidichimo, G. *Proc. SPIE* **1989**, *1080*, 32.

(11) Kitzerow, H.-S. *Liq. Cryst.* **1994**, *16*, 1.

(12) Denk, W.; Strickler, J. H.; Webb, W. W. *Science* **1990**, *248*, 73.

(13) (a) Springer, G. H.; Higgins, D. A. *J. Am. Chem. Soc.* **2000**, *122*, 6801. (b) Springer, G. H.; Higgins, D. A. *Chem. Mater.* **2000**, *12*, 1372.

10.1021/cm010185o CCC: $20.00
Published on Web 06/09/2001

In the materials described here, polymer microspheres are used to "prefabricate" or template[14,15] voids in the supporting polymer matrix. These voids are then loaded with liquid crystal. Materials containing randomly positioned droplets can be readily fabricated for conventional PDLC applications. Because the microspheres tend to self-organize to form colloidal crystals,[15,16] films comprised of well-ordered arrays of hexagonally packed liquid-crystal droplets can also be produced.

II. Experimental Considerations

A. Materials. Samples were prepared from commercially available poly(vinyl alcohol) (PVA), poly(ethylene glycol) (PEG), and nematic liquid crystal. The polymers were obtained from Aldrich and were used as received. Molecular weights (M_w) of PVA (96% hydrolyzed) and PEG were 100 000 and 8 000, respectively. Aqueous suspensions of commercially available carboxylate-terminated polystyrene microspheres (Interfacial Dynamics) were used for array preparation. Spheres of 0.5-, 1.1-, and 1.7-μm average diameters were used in different experiments. The polymers and microspheres were cast onto microscope cover slides. These substrates were rigorously cleaned prior to use by sonication in 3% NaOH, high-purity water (18 MΩcm), 2% H_2SO_4, and finally high-purity water. The nematic liquid crystal employed was a common eutectic mixture of cyanobiphenyls and terphenyls (E7) obtained from Merck. It also was used as received.

B. Microscopy. The polymer films were characterized during void array preparation by AFM. Contact mode AFM images were collected using conventional silicon nitride probes. Both Wyco and Digital Instruments Multimode atomic force microscopes were used. The liquid-crystal-filled polymer voids were characterized by MPE fluorescence microscopy,[12,13] using a sample-scanning confocal microscope.[13] In these experiments, ≈200 μW (average power) of 810-nm light from a mode-locked (170-fs pulse width, 76-MHz repetition rate) Ti:sapphire laser (Coherent Mira 900F, 5W Verdi pump) was directed into an inverted light microscope (Nikon) via a dichroic mirror (CVI Corporation). The light was focused to a diffraction-limited spot in the sample using a high-numerical aperture (NA = 1.3) 100X objective. Sample imaging and positioning was accomplished using a piezo-electrically driven stage (Queensgate) with closed-loop X,Y-feedback, giving ±3-nm positioning accuracy. Individual liquid-crystal molecules simultaneously absorb several photons from a single laser pulse and subsequently emit single fluorescence photons in the blue. Such methods provide high-resolution imaging and depth-profiling capabilities[17] with lateral resolution, R, given approximately by $R = 0.61\lambda/(n^{1/2}\mathrm{NA})$,[13] where n is the number of photons involved in the excitation process and λ is the incident wavelength. The 100X objective was also used to collect liquid-crystal fluorescence. It was subsequently passed back through the dichroic mirror and a band-pass filter (Chroma Technologies, 360−540-nm pass band) prior to detection with a photoncounting photomultiplier tube (Hamamatsu model HC135-01). MPE fluorescence spectra were obtained by directing the fluorescence into an imaging spectrograph (Acton Research) and onto a liquid-N_2-cooled charge-coupled-device (CCD) detector (Roper Scientific).

MPE in ordered dichroic materials is extremely sensitive to the polarization state of the incident light,[18] providing valuable information on liquid-crystal organization. Broadband half and quarter wave plates (Special Optics) were used to produce linear and circular polarization states, respectively (the former of arbitrary orientation), for polarization-dependent imaging experiments. Images recorded with circularly polarized excitation provide "total fluorescence" images, while liquid-crystal organization was studied using linearly polarized light.

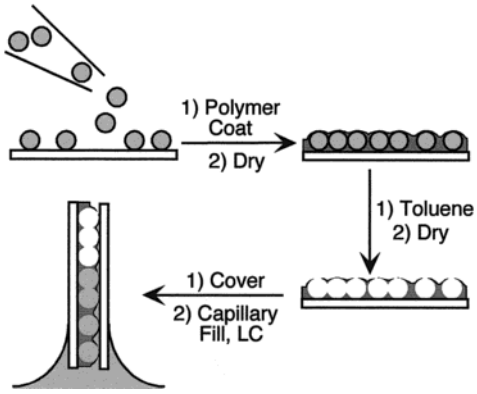

Figure 1. Procedure for fabrication of templated PDLC droplets and droplet arrays. Polystyrene microspheres are first deposited on a glass substrate. They are then coated with a water-soluble organic polymer. The spheres are subsequently extracted using organic solvent. The resulting polymer voids are then refilled with nematic liquid crystal using capillary action. For this procedure, the film is first covered with a second polymer-coated glass slide. Either ordered arrays or well-dispersed droplets may be formed.

III. Results and Discussion

A. Array Fabrication. Figure 1 depicts the overall film fabrication procedure. Thin films of carboxylate-terminated polystyrene microspheres were first deposited on glass microscope coverslips from aqueous suspensions. Both drop-casting and spin-casting procedures were employed to obtain monolayer and multilayer sphere arrays, depending on the sphere concentration in the suspension and/or the substrate spinning speed. Only monolayer films (i.e., two-dimensional arrays) were characterized here. The microsphere-coated substrates were dried in a 35 ± 5 °C oven for ≈24 h. They were subsequently coated with a thin film of PVA or PEG by spin casting from aqueous solution (3−10 wt %) and redried for ≈24 h. Figure 2A shows a contact-mode AFM image of an ordered, polymer-coated sphere array. As shown in the image, the addition of water-soluble polymer did not substantially disorder the arrays. Ordered regions as large as a few hundred microns in size were still observed. However, some of the spheres were removed during the coating procedure. Alternative methods are under development for obtaining more stable sphere arrays with more extensive array order.

The polystyrene spheres were subsequently dissolved from the films by dipping in toluene or chloroform for a period of 48 h. The films were oven-dried again for ≈24 h after removal from the solvent bath. Figure 2B shows an AFM image of the templated voids left behind in the polymer (PVA or PEG) films. Final polymer film thickness (total height of the polymeric features) was determined by AFM and was found to increase with increasing polymer concentration in the coating solution. Films prepared from 3% and 10% polymer solutions were nominally 300 nm and 1 μm (±200 nm) thick, respectively. Polymer networks were found in densely packed,

(14) Holland, B. T.; Blanford, C. F.; Stein, A. *Science* **1998**, *281*, 538.
(15) Johnson, S. A.; Ollivier, P. J.; Mallouk, T. E. *Science* **1999**, *283*, 963.
(16) Weissman, J. M.; Sunkara, H. B.; Tse, A. S.; Asher, S. A. *Science* **1996**, *274*, 959.
(17) Gu, M. *Opt. Lett.* **1996**, *21*, 988.
(18) McClain, W. M. *J. Chem. Phys.* **1974**, *57*, 2264.

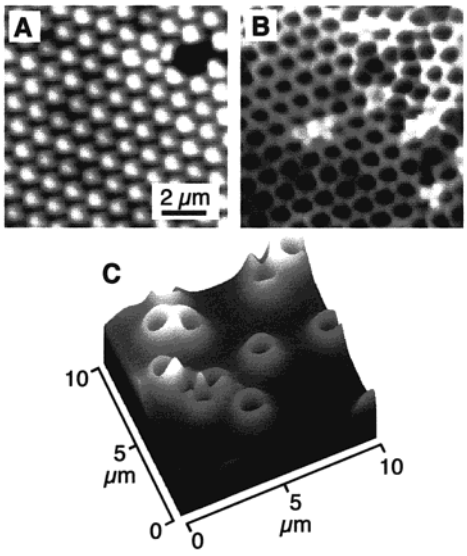

Figure 2. Topographic images of the samples at intermediate steps during film fabrication. (A) Image of PVA-coated 1.1-μm polystyrene spheres on a glass substrate. (B) PVA network and void arrays remaining after extraction of the spheres. (C) Well-dispersed voids in PVA (prepared from 3% PVA solution). All images shown were recorded by contact-mode AFM. Total height variation depicted by the gray scale is ≈300 nm in each image.

hexagonally ordered and disordered regions for both PVA and PEG materials. The formation of these networks is consistent with the penetration of polymer solution into the interstitial voids between the polystyrene spheres. Wetting of the spheres by the polymer solution facilitates this process. Syntheses of similar meso- or macroporous materials from colloidal arrays have been widely described in the literature.[4,14−16,19] In several reports, the interstitial voids were filled using polymeric precursors,[15,19] or polymer melted from the shells of core−shell composite spheres.[20]

To better understand film formation, interactions between the matrix polymer and spheres, and resulting film morphology, samples containing well-dispersed voids were also prepared and imaged. Crater-like structures were observed in such samples prepared with PVA, as shown in Figure 2C. The "crater" morphology results from the wetting of the carboxylate-terminated polystyrene sphere surfaces by polymer solution. The results are consistent with a relatively low contact angle between PVA and the sphere surfaces and support the proposed mechanism for network formation. In images of similar samples prepared with PEG, the raised "ridge" around each void was significantly smaller, indicative of a greater contact angle and reduced wetting of the microsphere surfaces. The observed film morphology in both cases provides evidence as to the mechanism by which the microspheres are removed from the film. The AFM images and film thickness data suggest that the larger spheres were not completely covered by polymer (PEG or PVA). However, as the AFM probe imparts substantial forces on the sample surface, it is also possible the voids were originally covered by a thin polymer membrane that was removed or destroyed during imaging. It is more likely that relatively large openings (as shown in the AFM images) in the polymer film are actually left at the top of each sphere. Indeed, AFM measurements indicate the void depths are only approximately 800 nm, or about 50% of the sphere diameter for the largest (1.7 μm) spheres, when 10% polymer solutions are employed. Such openings would result from incomplete wetting of the sphere surface by the aqueous polymer solution and/or polymer film shrinkage during drying. Despite these uncertainties, the results indicate that extraction of the polystyrene requires, at most, its diffusion through a very thin covering polymer film. As a result, sphere extraction is facile and not substantially hindered by the surrounding polymer.

Following chemical removal of the microspheres, the voids were refilled by nematic liquid crystal. In this step, a second glass substrate was used to cover the film. The cover glasses used had been previously coated with a thin film of the matrix polymer and dried. In some cases, the polymer-coated substrates were rubbed with a cloth along a well-defined direction to induce liquid-crystal alignment (see below). The primary purpose of this polymer coating was to provide "uniform" interfacial conditions around the entire droplet circumference. The covering slide and substrate were clamped and/or cemented together and the polymer voids refilled by capillary action (Figure 1).[21]

Figure 3 shows polarization-dependent MPE fluorescence images of ordered sphere arrays. Figure 4 shows the power dependence and spectral characteristics of liquid-crystal fluorescence excitation and emission. The MPE fluorescence data in Figure 4 were recorded for individual droplets similar to those shown in Figure 3. The log−log plot of fluorescence counts versus incident power has a slope of 2.8. The average of several such measurements yielded a slope of 2.9 ± 0.1. These results indicate the excitation process involves absorption of three photons of 810-nm light by the sample. As shown in Figure 4, the one-photon liquid-crystal excitation spectrum is peaked near 275 nm. The resulting emission occurs in a broad band centered near 390 nm. This emission arises in part from the formation of excimers in the nematic phase.[22] The uncorrected three-photon-excited fluorescence spectrum (see Figure 4) recorded by spectrally dispersing the emission from a single liquid-crystal droplet closely parallels this spectrum, proving the fluorescence comes from the liquid crystal. The structure in the spectrum is caused by the optical filters employed.

Fluorescence images recorded with circularly polarized excitation provide the best view of the liquid-crystal-filled voids, as shown in Figure 3A. Fluorescence signals from the droplets are typically in the 10^5 counts/s range and peak over the center of each droplet. This signal is 100 times larger than that obtained from the polymer networks prior to being filled with liquid crystal. The images clearly show that the droplets

(19) (a) Asher, S. A.; Holtz, J.; Liu, L.; Wu, Z. *J. Am. Chem. Soc.* **1994**, *116*, 4997. (b) Park, S. H.; Xia, Y. *Chem. Mater.* **1998**, *10*, 1745.
(20) Kumacheva, E.; Kalinina, O.; Lilge, L. *Adv. Mater.* **1999**, *11*, 231.
(21) Kim, E.; Xia, Y.; Whitesides, G. M. *Nature* **1995**, *376*, 581.
(22) Subramanian, R.; Patterson, L. K.; Levanon, H. *Chem. Phys. Lett.* **1982**, *93*, 578.

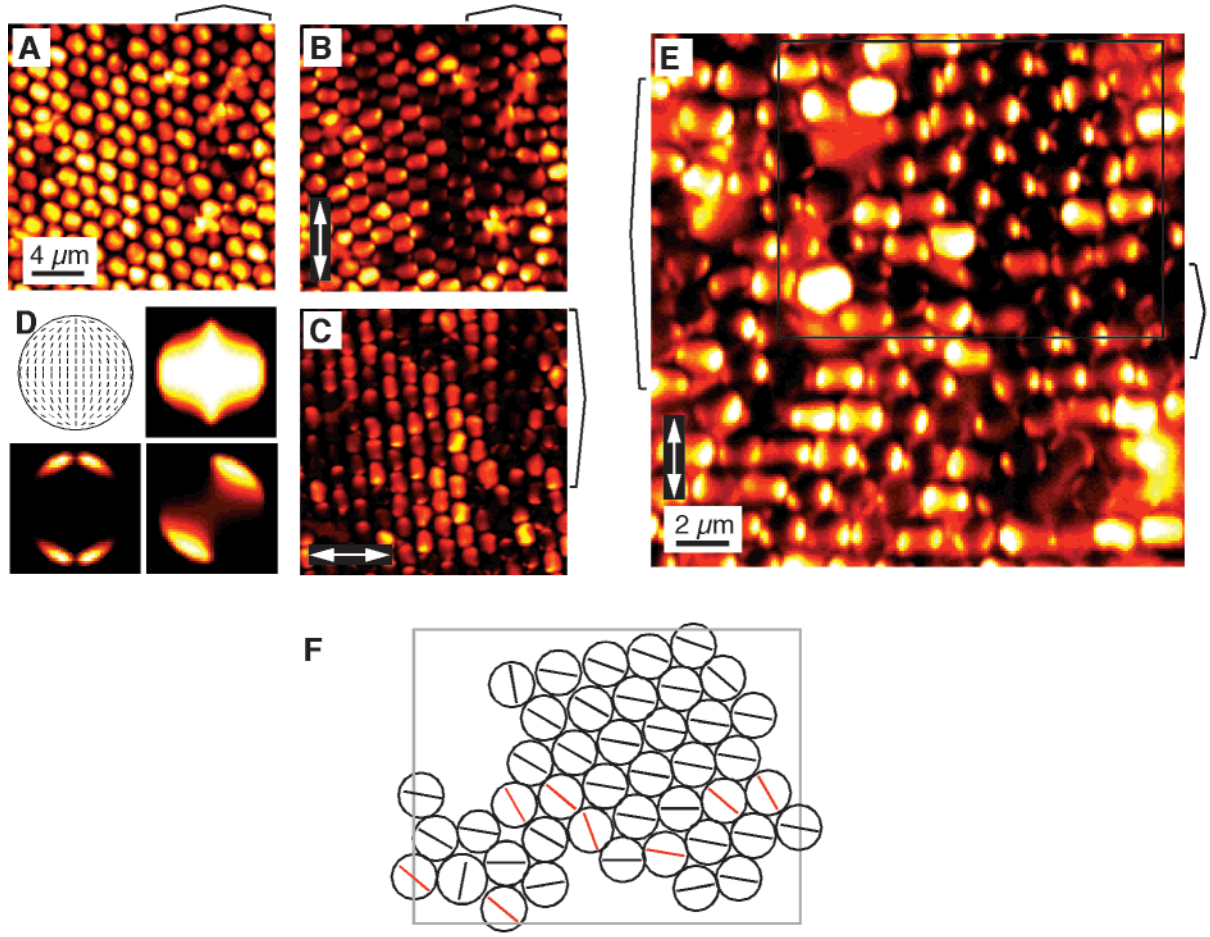

Figure 3. (A−C) MPE fluorescence images of liquid-crystal droplet (1.7-μm-diameter) arrays in a PEG film recorded under different polarization conditions. The color scale depicts photon count rates between 10^3 s^{-1} (black) and 10^5 s^{-1} (white). The color scales are identical in (B) and (C). (A) Fluorescence excited with circularly polarized light, showing the well-ordered liquid-crystal-filled arrays. (B) and (C) The same region excited with linearly polarized light (appended arrows show the polarization). (D) Shown (clockwise) are simulations of the nematic organization and three-photon-excited fluorescence images in 2-μm-diameter droplets for linearly polarized excitation parallel, at 45°, and perpendicular (contrast-enhanced) to the nematic axis. Instrument resolution was simulated by convolution of the results with a 250-nm Gaussian function. (E) Fluorescence image (contrast-enhanced) of a different sample region showing clear long-range organizational correlations between droplets. Transitional and defected regions are highlighted by the brackets. (F) Approximate in-plane alignment of the polar axes for the droplets within the box in (E) determined from simulations (see (D)). Errors in the orientation estimates (black) are ±15°. The red axes denote ambiguous alignments (cases near 45°) for which an axis orientation rotated in the opposite sense with respect to the incident polarization would yield a similar image.

formed are of uniform size and form a well-ordered hexagonal array in many regions. For materials applications, it is particularly important that droplet size can be altered by simply changing the size of the microspheres used in film preparation. Only 1.7-μm-diameter droplet arrays are shown here because the optical features described below could not be properly resolved for the 0.5- and 1.1-μm-diameter droplets. It should be noted that a fluorescent "haze" or background is observed in some images. The haze comes from small amounts of liquid crystal that is not entrapped within the voids. By a simple change in the microscope focus (i.e., in depth-profiling studies), it is readily shown that this liquid crystal is likely trapped between the polymer void array and the polymer-coated covering glass surface.

B. Liquid-Crystal Organization. Liquid-crystal organization within individual droplets is investigated by recording images under different excitation polarization conditions. The utility of such experiments results in part from the strong polarization dependence of multiphoton excitation.[18] Importantly, the strong, lowest energy electronic transitions in the liquid-crystal molecules are expected to be well-polarized along the long molecular axis (i.e., the nematic axis). Numerous studies of substituted biphenyls have shown this to be the case for one-photon excitation.[23] As a first-order approximation, it may then be assumed that a single element of the nonlinear polarizability tensor[18] dominates for three-photon excitation in this spectral region (810 nm). Most efficient excitation occurs when all three incident photons are polarized parallel to the local transition dipole and a $\cos^6 \theta$ dependence on the incident polarization angle is predicted. Here, θ is the angle between the transition dipole (parallel to the local nematic axis) and the incident polarization vector.

From the polarization-dependent data presented in Figure 3, it is clear that fluorescence excitation is indeed highly dependent on incident polarization. The fluores-

(23) (a) Maus, M.; Rettig, W. *Chem. Phys.* **1997**, *218*, 151. (b) Platt, J. R. *J. Chem. Phys.* **1951**, *19*, 101.

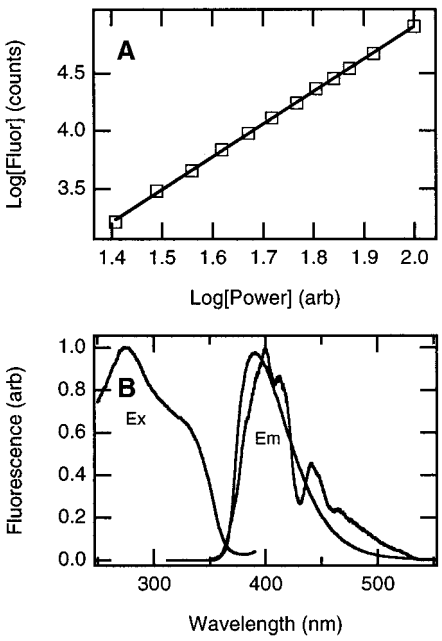

Figure 4. (A) Log−log plot showing the dependence of liquid-crystal fluorescence on incident power at 810 nm. The plot has a slope of 2.8. (B) One-photon fluorescence excitation (400-nm emission) and resulting liquid-crystal emission (340-nm excitation) spectra for thin-film samples on a quartz substrate. Also shown is the uncorrected fluorescence spectrum (structured curve) recorded for a single droplet by three-photon excitation at 810 nm.

cence signal varies by a factor of ≈20 as the incident polarization (linear) is rotated through 180°. These data indicate the liquid crystal is present in a well-ordered state and that the electronic transition participating in excitation of the molecules is well-polarized, likely along the long molecular axis as expected.[23] The polarization-dependent "patterns" observed for each individual droplet then provide detailed information on local liquid-crystal alignment. It is conclusively demonstrated by these images that the liquid-crystal molecules are aligned parallel to the void surfaces. These results confirm that the preparation procedure (particularly the use of polystyrene microspheres and their subsequent extraction) has not changed the expected nematic anchoring conditions at the interface.[11] Under such circumstances, for the samples studied here, the liquid crystal is expected to assume the well-known "bipolar" organization.[11]

Figure 3D shows two-dimensional simulations of bipolar nematic organization and the droplet images expected under different excitation polarizations.[24,25] As is most clearly shown in Figure 3E, a large number of droplets yield fluorescence patterns very similar to the simulated images (Figure 3D). For example, the bright (highly fluorescent) droplet near the lower left corner of the black box superimposed in Figure 3E has an appearance similar to that expected for fluorescence excitation with light polarized parallel to the polar axis (upper right image in Figure 3D). Similarly, a large number of droplets just to the right of center near the top of Figure 3E mimic the "four-lobed" patterns expected for excitation with light polarized perpendicular to the polar axis (lower left image in Figure 3D). These results indicate the liquid crystal is indeed organized in the bipolar configuration. Comparison of the experimental and simulated data then allows for the average nematic alignment in each droplet (corresponding to the droplet optical/polar axis alignment) to be deduced. Figure 3F gives the approximate polar axis alignment for several droplets shown in Figure 3E. The images also indicate that the polar axes of virtually all droplets observed are aligned very close to parallel to the substrate surface (i.e., in the film plane). This is likely a result of the nonspheroidal nature of the droplet voids obtained. That is, the spheroidal cavities are likely truncated near the upper film surface (as evidenced by the AFM images above), giving the droplets a nominally "flat" top when covered by the second slide. As a result, alignment parallel to the film plane is induced. In more traditional systems,[11] nearly spheroidal liquid-crystal droplets of random orientation with respect to the film plane are often obtained.

Much more interesting than the determination of liquid-crystal alignment in individual droplets is the observation of unexpected, yet clearly apparent, "long-range" organizational correlations between droplets in some sample regions. That is, the alignment of the individual droplet polar axes are often observed to be similar for neighboring droplets. Subtle evidence for these correlations are depicted by the "light" and "dark" regions in the fluorescence images shown in Figure 3B,C. The color scale in these images primarily reflects the efficiency of fluorescence excitation, which in turn is strongly dependent on the local liquid-crystal orientation. It may then be concluded that the polar axes of the droplets that appear relatively brighter are more closely aligned with (parallel to) the incident polarization. Thus, the relatively large light regions in this figure correspond to domains containing droplets of similar polar axis alignment. The same may be said for the dark regions. Figure 3E,F shows a particularly clear example of domain formation. Again, the distinctive polarization-dependent patterns predicted for perpendicularly polarized excitation (Figure 3D) are readily observed (albeit rotated by 90°) for a number of droplets (approximately 16) found near the top and just to the right of center in Figure 3E. The polar axes of all the droplets in this domain are approximately oriented along the horizontal direction in the image.

The observed organizational correlations could have several origins. Slight distortions in the droplet shapes brought about by extension and/or compression of the array along any particular axis may play an important role. Such film morphological attributes are indeed known to cause alignment in purposefully "shaped" droplets prepared by other means.[10] In droplets of slightly elongated shape, minima exist in the organizational free energy[25] such that alignment of the polar axis either parallel or perpendicular to the elongation axis may occur. Also possible is the coupling of droplet organization through channels formed in the polymer network. Such channels likely form at the original contact points of the polystyrene spheres. If these channels are relatively large, the nematic alignment from one droplet may be effectively "transmitted" to its

(24) Zumer, S.; Doane, J. W. *Phys. Rev. A* **1986**, *34*, 3373.
(25) Ondris-Crawford, R.; Boyko, E. P.; Wagner, B. G.; Erdmann, J. H.; Zumer, S.; Doane, J. W. *J. Appl. Phys.* **1991**, *69*, 6380.

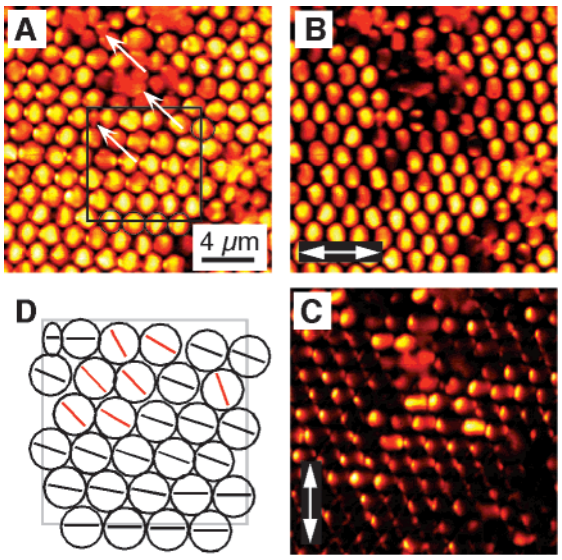

Figure 5. (A−C) MPE fluorescence images of a well-ordered droplet array in a sample where liquid-crystal alignment was induced along the horizontal direction in the images by rubbing the polymer-coated covering glass slide. The color scale depicts photon count rates between 10^3 s^{-1} (black) and 10^5 s^{-1} (white). The color scales are identical in (B) and (C). (A) Sum of the images shown in (B) and (C), which were excited with the linear polarizations shown. (D) Approximate in-plane alignment of the polar axes for the droplets within the box in (A). Except in defected regions, the polar droplet axes are aligned predominantly parallel to the rubbing direction.

neighbors. It is also possible the liquid crystal is aligned by flow during capillary filling, with alignment predominantly parallel to the flow direction. Last, because the droplets may be in contact with the polymer coating on the covering glass slide, any structural features in the covering film may also induce liquid-crystal alignment. It is likely all these mechanisms contribute to some degree.

To investigate the dependence of alignment on the morphology of the covering polymer film, samples were prepared using covering films that had been rubbed along a well-defined direction. Example images recorded for such samples are shown in Figure 5. The rubbing direction in this sample is parallel to the horizontal direction on the images. It is clearly apparent from Figure 5 that the polar axes in the vast majority of droplets are aligned parallel to the rubbing direction. Parallel alignment is observed for well-ordered hexagonal regions, regardless of how the droplet rows in the hexagonal domains are oriented with respect to the rubbing direction. These results conclusively prove the importance of the polymer-coated cover glass in determining liquid-crystal alignment in the two-dimensional droplet arrays studied here. They also prove that the majority of liquid-crystal voids in monolayer samples are not completely covered by the polymer comprising the void array matrix. An opening in the film must occur at the top of most voids, as observed above in the AFM images.

Importantly, alignment parallel to the rubbing direction is not always observed. Near the center of the region shown in Figure 5, several droplets exhibit substantially different liquid-crystal alignment (see Figure 5D for examples). These deviations appear to occur primarily near distortions in the hexagonal array. Such distortions arise from single- or multiple-void defect sites and other domain boundaries. In this region there appear to be several extra droplets (see arrows in Figure 5A) that distort the array. Deviations from the rubbing-induced alignment occur in the nearby voids. It is noteworthy that macroscopic alignment on much larger centimeter length scales could be readily induced in films prepared by sandwiching liquid crystal between two rubbed, void-free polymer-coated substrates. Therefore, it is likely that subtle distortions in the droplet shape resulting from defect-induced extension/compression of the void array cause the observed alignment deviations. Droplet shape becomes the dominant factor in determining liquid-crystal organization in such distorted droplets.

Numerous regions exhibiting significantly more array disorder have also been imaged in both rubbed and unrubbed samples. The results point clearly to the influences of droplet shape on alignment. Although not shown, most disordered regions exhibit liquid-crystal alignment variations similar to those shown in the center of Figure 3E and on the right-hand side of Figure 3A−C (unrubbed samples). Liquid-crystal alignment varies dramatically between neighboring voids in these regions. Alignment in regions showing similar disorder in rubbed samples is similarly independent of the rubbing direction, indicating array disorder must be the cause of observed orientational variations. Such effects are expected in regions where droplet shape dominates over other liquid-crystal alignment mechanisms. Unfortunately, the exact nature of the array distortions (i.e., the direction of array extension/compression) are difficult to deduce at present. These difficulties arise primarily because of the apparently subtle nature of the droplet shape variations that lead to changes in liquid-crystal alignment.

The contributions of the channel and flow mechanisms are unclear at present. However, it is believed these mechanisms are less important. Array order should not play such an important role if liquid-crystal alignment is predominantly controlled by “transmission” of the liquid-crystal orientation through channels between the voids. Such channels are expected to form between contacting voids, regardless of local void organization. As such, even defected regions should show long-range correlations. While such correlations are observed, they usually occur in regions where alignment of the hexagonal array varies slowly over several voids (see the center right-hand side of Figure 3E). In highly defected regions and at discrete domain boundaries, liquid-crystal alignment tends to change dramatically between droplets, indicating local alignment is not transmitted across the boundary. The flow mechanism may also be discounted as a major contributor. Were such a mechanism important, strong alignment similar to that observed in Figure 5 would be expected in unrubbed samples. The observation of slow orientational variations across large ordered domains like those shown in Figure 3A−C is inconsistent with macroscopic flow-induced alignment. However, it is an interesting possibility that formation of such domains could result from complex microscopic flow paths taken by the liquid crystal during capillary filling. The detailed mechanism for domain ordering and changes in liquid-crystal align-

ment across domain boundaries are currently under investigation. It is clear, however, that array order plays a very important role in the alignment mechanism, likely via subtle distortions in droplet shape.

IV. Conclusions

The preparation of PDLC films with highly controlled droplet sizes and shapes has been accomplished using a droplet templating procedure. This method represents an important alternative to procedures presently used in PDLC fabrication and will likely lead to the development of optical devices with enhanced properties. For example, new electrically switchable diffractive optics having applications as optical filters may be fabricated from well-ordered three-dimensional hexagonal droplet arrays that may be prepared by similar methods. Aside from the potential technological importance of these methods, unexpected physical phenomena were also uncovered. Namely, surprising long-range orientational correlations were observed in domains of neighboring liquid-crystal droplets. Such correlations were found predominantly in regions of well-ordered, hexagonally arranged droplets. It was shown that the morphology of the covering polymer surface plays a significant role in determining liquid-crystal alignment and can cause such correlations. It was also proposed that long-range correlations may result from slight distortions in the droplet shape due to expansion/compression of the hexagonal droplet arrays. The importance of droplet shape variations in disrupting these long-range orientational correlations was also observed. In the future, the origins of such phenomena will be explored in more detail. The results will provide a much better understanding of subtle variations in array order and void shape in these and similar meso- or macroporous systems.

Acknowledgment. This work was supported by the National Science Foundation (CHE-9701509, CHE-9709034, CHE-0092225, and DMR-0076169). Additional financial support was obtained from 3M Corporation. Maryanne Collinson, Ken Klabunde, and their respective research groups at Kansas State University are thanked for their contributions to these studies.

CM010185O